International Journal of Applied Science and Engineering

Optimizing friction stir welding parameters for enhanced mechanical properties of dissimilar aluminum alloys AA5083 and AA6063: A Taguchi approach

Sittichai Charonerat [1], Thanatep Phatungthane [2], Chuthong Summatta [1*]

[1] *Industrial Technology, Nakhon Phanom University, Nakhon Phanom 48000, Thailand*
[2] *Division of Science, Faculty of Education, Nakhon Phanom University, Nakhon Phanom, 48000, Thailand*

ABSTRACT

This study aims to optimize Friction Stir Welding (FSW) parameters to improve the mechanical properties of AA5083-AA6063 aluminum alloy joints, which are crucial for applications requiring high strength and durability. A Taguchi L9 orthogonal array experimental design was employed to systematically vary three key parameters: rotation speed, travel speed, and tool-pin taper angle, with the objective of maximizing tensile strength and hardness. The results demonstrated that a moderate rotation speed combined with a larger tool-pin taper angle produced optimal outcomes, achieving a tensile strength of 215.40 MPa and a hardness of 90.69 HV. Statistical analyses using signal-to-noise ratios and Analysis of Variance (ANOVA) identified rotation speed as the most influential factor affecting both tensile strength and hardness, followed by tool-pin taper angle, while travel speed had a minimal impact. Microscopic examinations revealed that the optimized settings yielded defect-free welds with ductile fracture patterns. These findings underscore the critical importance of precise FSW parameter selection in enhancing weld quality and contribute valuable insights for advanced manufacturing applications in industries requiring robust aluminum alloy joints.

Keywords: FSW, Dissimilar Aluminum alloys, Mechanical properties, Taguchi approach

OPEN ACCESS

Received: November 21, 2024
Revised: April 18, 2025
Accepted: September 1, 2025

Corresponding Author:
Chuthong Summatta
Chuthong@npu.ac.th

Publisher:
Chaoyang University of Technology
ISSN: 1727-2394 (Print)
ISSN: 1727-7841 (Online)

1. INTRODUCTION

Advancements in welding techniques have significantly expanded the capabilities for creating robust and durable joints in engineering materials; however, challenges persist, particularly when joining dissimilar aluminum alloys. Optimizing welding parameters is critical in applications demanding high mechanical strength and durability, such as those in the automotive, aerospace, and marine industries. Dissimilar alloys like AA5083 and AA6063 possess distinct mechanical properties and chemical compositions, complicating the welding process and potentially compromising weld quality and joint integrity. Specifically, AA5083 is renowned for its strength and excellent corrosion resistance, making it suitable for marine environments, whereas AA6063 is valued for its formability and extrudability, commonly utilized in structural applications. These differing properties necessitate meticulous optimization of welding parameters to ensure that the resulting joint meets the mechanical demands of its intended application (Elnabi et al., 2019; Umanath et al., 2021). However, welding AA5083 and AA6063 together presents unique metallurgical and mechanical challenges due to their significantly different thermal properties and alloy compositions. The disparity in thermal conductivity, melting temperatures, and flow behavior during friction stir welding (FSW) can lead to uneven heat distribution and inconsistent material mixing in the stir zone. These differences often result in the formation of defects such as voids, tunnel defects, or weak interfacial bonding, which degrade the mechanical performance of the welded joint. Therefore, precise control of FSW parameters is essential to minimize these effects and ensure the formation

of high-quality dissimilar joints.FSW emerges as a particularly effective method for joining aluminum alloys due to its ability to produce high-quality welds without melting the base materials, thereby preserving their desirable properties. This solid-state process is highly relevant in industries where joint performance is paramount, enabling applications that require both strength and ductility. For dissimilar aluminum alloys such as AA5083 and AA6063, FSW offers an innovative solution; however, achieving optimal joint properties depends on carefully tuning parameters like rotation speed, travel speed, and tool-pin taper angle to avoid defects and ensure uniformity. Although several studies have investigated FSW parameters for both individual alloys and dissimilar aluminum combinations, limited research has focused specifically on optimizing the process for the AA5083-AA6063, few research have employed systematic multi-parameter optimization techniques such as the Taguchi method specifically for AA5083-AA6063 joints. Moreover, many previous studies have focused solely on tensile properties without correlating them with microstructural analysis or The studies lacked statistical robustness in identifying optimal process windows. Additionally, some works applied full factorial designs or single-variable studies, which may not efficiently reveal interaction effects among critical parameters Elatharasan et al. (2020). These gaps highlight the need for an integrated approach combining statistical design, mechanical testing, and microstructural validation, which this study aims to provide.

The research gap in optimizing FSW parameters for dissimilar aluminum alloys remains largely unaddressed, particularly concerning AA5083 and AA6063. The scarcity of systematic studies on dissimilar joints between these alloys and the lack of consistent methodologies underscore the need for research that leverages robust optimization techniques. The Taguchi method, a powerful statistical tool for optimizing processes with multiple parameters, has shown promise in FSW studies but has been underutilized for dissimilar AA5083-AA6063 joints (Elnabi et al., 2019; Umanath et al., 2021).

This study aims to optimize FSW parameters for AA5083-AA6063 dissimilar joints to enhance key mechanical properties such as tensile strength and hardness, employing the Taguchi L9 orthogonal array design. By providing insights into the effects of parameter settings on joint performance, this research seeks to contribute to improved manufacturing practices and guidelines for achieving high-performance aluminum alloy joints, with potential applications across industries that prioritize durability and reliability.

Mechanical Properties of Dissimilar Aluminum Alloy Joints in FSW. Recent advancements in FSW have highlighted the critical role of welding parameters and material enhancements in optimizing the mechanical properties of dissimilar aluminum alloy joints, particularly AA5083 and AA6063. FSW's solid-state joining mechanism allows for control over thermal input, minimizes defects, and enhances joint quality. Studies have shown that precise adjustments of parameters like tool rotational speed, welding speed, axial force, and tool geometry significantly impact tensile strength, hardness, grain size, and microstructure of the joints (Okubo et al., 2007; Patel et al., 2019; Serier et al., 2019; Balamurugan et al., 2023). Incorporation of nanoparticle reinforcements, such as La_2O_3, has further enhanced these properties, achieving superior tensile strength and hardness (Arun et al., 2021). Comparative analyses using predictive models and response surface methodology have facilitated the optimization of FSW parameters for different aluminum alloys, addressing challenges in achieving consistent mechanical properties across dissimilar alloys (Al-Sabur, 2021; Lewise et al., 2023). These findings underscore FSW's suitability for producing high-quality, durable aluminum joints required in advanced automotive and aerospace applications, emphasizing the importance of precise parameter control and innovative approaches in advancing high-performance applications.

Influence of FSW Parameters on Weld Quality and Microstructure. The quality and microstructure of FSW joints, especially in aluminum alloys like AA5083 and AA6063, are profoundly influenced by key parameters-rotation speed, travel speed, and tool geometry-that control heat input, plastic deformation, and material flow within the weld zone, directly affecting mechanical properties (Serier et al., 2019; Al-Sabur, 2021; Balamurugan et al., 2023). Optimizing rotation speed is crucial; while higher speeds increase frictional heat and improve plastic flow, excessively high speeds can cause overheating and grain coarsening, compromising mechanical integrity (Balamurugan et al., 2023). Similarly, travel speed dictates heat application duration and cooling rates; careful modulation can yield finer grains and enhance hardness, but too rapid speeds may result in incomplete bonding (Serier et al., 2019). Tool geometry, including shoulder diameter and pin profile, significantly affects material flow and heat distribution, with specific configurations promoting superior grain refinement and consistent microstructure across the joint (Al-Sabur, 2021). Understanding the

Table 1. Chemical composition and mechanical properties of AA5083 and AA6063

Materials	Element (%wt)									Mechanical test	
	Al	Mg	Zn	Ti	Fe	Si	Mn	Cu	Cr	Ts (MPa)	Hv
AA5083	Bal.	4.27	0.02	0.026	0.31	0.1	0.61	0.04	-	273.79	82
AA6063	Bal.	0.67	0.05	0.080	0.30	0.45	0.10	-	-	210.35	63

sensitivity of these parameters allows for precise control over microstructural evolution and mechanical behavior, forming the basis for optimizing FSW conditions to achieve high-quality joints in dissimilar aluminum alloys.

Applications of Taguchi Method in Welding Process Optimization. The Taguchi method is a powerful statistical approach for optimizing complex, multi-parameter processes like FSW, where parameters such as rotation speed, travel speed, and tool geometry dynamically affect weld quality. By employing orthogonal array designs, it systematically evaluates parameter interactions, enabling researchers to identify optimal conditions with fewer experimental trials-particularly advantageous in resource-intensive welding processes. Studies by Al-Sabur (2021) demonstrated that specific combinations of tool rotation and travel speed significantly enhance tensile strength and hardness in aluminum alloys while. Balamurugan et al. (2023) showed that maximizing the signal-to-noise (S/N) ratio in Taguchi-based FSW optimization achieves consistently high-quality joints across varied environmental settings. The method's robustness in handling noise factors and simplifying the identification of main effects and interactions among parameters makes it invaluable for optimizing joint properties in dissimilar alloys like AA5083 and AA6063. Its ability to streamline multi-parameter optimization while controlling for external influences provides a solid foundation for the present study, which seeks to establish optimized welding parameters for producing high-quality dissimilar aluminum alloy joints.

2. MATERIAL AND METHOD

2.1 Experimental Material

In this study, the mechanical properties of aluminum alloys AA5083 and AA6063 were investigated and compared after undergoing the FSW process. These materials were selected due to their significantly different properties, which are expected to influence the weld quality and mechanical characteristics of the joint. AA5083 is an aluminum alloy primarily composed of magnesium and manganese, known for its high strength and excellent corrosion resistance, making it suitable for marine applications. Conversely, AA6063 is an aluminum alloy containing magnesium and silicon, offering good formability and extrudability, making it ideal for structural and architectural components. The chemical composition and mechanical properties of AA5083 and AA6063 are shown in Table 1. Both materials, with dimensions of 150 x 75 x 6 mm, were prepared by bandsaw cutting, followed by edge milling with a CNC machine to ensure high-quality contact surfaces. The samples were then cleaned with acetone to remove contaminants and oil residues. This meticulous specimen preparation process is crucial, as it directly affects the welding performance and mechanical properties of the resulting joint.

2.2 FSW Process and Mechanical Testing

The experimental setup for evaluating FSW parameters on the mechanical properties of AA5083 and AA6063 aluminum alloys is illustrated in Fig. 1. The welding tool, made from hardened SKD11 steel, was mounted on a high-speed spindle to perform the FSW process. The tool used in this study was fabricated from hardened SKD11 tool steel and featured a cylindrical shoulder and a tapered pin. The shoulder diameter was 16 mm, while the pin was 5 mm. long and conically shaped. The tool tilt angle was adjusted at 0°, 3°, and 6°, and its total tool height was 40 mm. The conical pin design was intended to promote effective material flow and stirring during the welding process. These geometrical specifications were selected to ensure sufficient heat generation, proper material consolidation, and compatibility with 6 mm thick workpieces. This setup ensures that the tool and workpiece are securely held by precision fixturing and jigs, providing stability and accuracy during welding. As shown in Fig. 1(a), the tool rotation side (RS) and advancing side (AS) are aligned with the welding direction, allowing controlled heat generation and material flow. The study investigates the effects of three primary FSW parameters on the resulting mechanical properties of the weld joint. The rotation speed (S) of the tool is varied at three levels: 800, 900, and 1000 rpm, which influences the amount of heat and material flow. The travel speed (F), set at 20, 40, and 60 mm/min, impacts the exposure time and thermal profile along the weld line. Additionally, as illustrated in Fig. 1(b), the tool-pin taper angle (A) is adjusted between 0°, 3°, and 6°, with variations in the taper angle affecting the stirring and consolidation of the material in the weld zone.

This experimental setup aims to determine the optimal combination of FSW parameters that enhance the mechanical properties of AA5083-AA6063 welded joints. The findings will contribute to improved tool design and process optimization for high-performance aluminum alloy welding applications, particularly in advanced manufacturing contexts.

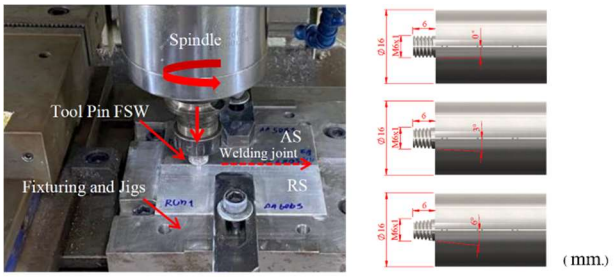

Fig. 1. The FSW process: (a) welding and clamping setup, (b) Welding tool

Fig. 2 illustrates the preparation of test specimens for mechanical property evaluation and microstructural analysis of the welded joint. The welded plate consists of AA5083 and AA6063 aluminum alloys, joined through the FSW process. The specimens are prepared according to

precise dimensions to enable different testing methods, including tensile strength and hardness tests, following standardized protocols. The tensile test specimens are prepared in accordance with ASTM E8M standards to ensure reliable and comparable measurements of mechanical properties. Hardness testing is conducted following ASTM E384 standards, with testing points strategically positioned along the weld zone to evaluate the variation in hardness across the joint. For microstructural analysis, specimen preparation adheres to ASTM E407 standards, allowing a detailed examination of the weld and heat-affected zones using a Scanning Electron Microscope (SEM).

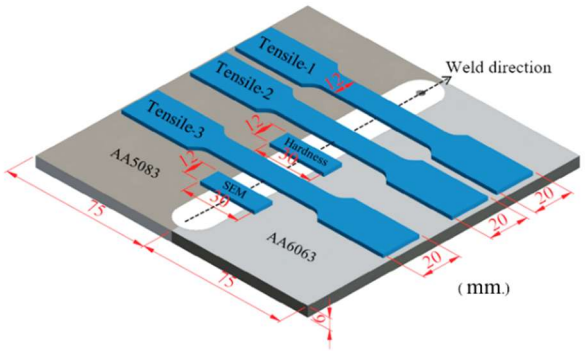

Fig. 2. Preparation of specimens for mechanical testing and microstructural investigation

2.3 Experimental Design

To optimize the FSW parameters for the mechanical properties of AA5083 and AA6063 alloys, a Taguchi experimental design approach was utilized. This method is widely recognized for its efficiency in systematically evaluating the effects of multiple factors on output characteristics, making it ideal for improving tensile strength and hardness in welded joints. The experimental design included three primary factors: Rotation Speed (S), Travel Speed (F), and Tool-Pin Taper Angle (A). These parameters were abbreviated in the array and figures as S (rpm), F (mm/min), and A (degrees), respectively. Each factor was studied at three levels, as shown in Table 2: S levels of 800, 900, and 1000 rpm; F levels of 20, 40, and 60 mm/min; and A levels of 0°, 3°, and 6°. An L9 orthogonal array was selected to balance the experimental load with the need for robust data analysis. This array allows for an efficient exploration of the parameter space while minimizing the number of experimental runs. Orthogonal arrays (OAs) are structured experimental designs that allow the simultaneous study of multiple parameters and their effects using a reduced number of trials. Each combination of parameter levels is arranged in such a way that all factors are statistically independent of each other. This independence ensures balanced comparisons and minimizes experimental bias. In this study, the L9 OA enabled the investigation of three parameters at three levels each, reducing the total number of experiments from 27 (full factorial) to just 9 while maintaining analytical rigor. This makes the Taguchi method highly efficient, particularly for resource-intensive processes like welding.

Table 2. Process parameters values and their levels.

Parameters	Level 1	Level 2	Level 3
Rotation speed (rpm)	800	900	1000
Travel speed (mm/min)	20	40	60
Tool-pin taper angle (θ°)	0	3	6

In this study, tensile strength and hardness were identified as the key responses. Since the aim was to maximize these mechanical properties, the "larger is better" criterion was applied within the Taguchi methodology. The "larger is better" S/N ratio for each experiment can be calculated using the following equation (1)

$$S/N_{Ratio} = -10\log\left(\frac{1}{n}\sum_{i=1}^{n}\frac{1}{y_i^2}\right) \quad (1)$$

where n is the number of observations in each experimental run, and y_i represents the individual measured values of tensile strength or hardness. This equation is particularly useful for maximizing the response by minimizing variability.

The data collected from the experiments were analyzed by calculating the S/N ratios for each response to determine the optimal parameter combination that enhances joint performance. The S/N ratios allow for identifying the influence of each parameter on the responses, thereby aiding in achieving a robust welding process. By comparing the average S/N ratios for each level of the factors, the optimum parameter settings can be identified to maximize tensile strength and hardness of the welded joint.

3. EXPERIMENTAL RESULT

3.1 Optimization by Taguchi

Table 3 illustrates the application of a Taguchi L9 orthogonal array design employed to optimize FSW parameters for enhancing the mechanical properties—specifically tensile strength (Ts) and hardness (Hv)—of AA5083-AA6063 alloy joints. Three key process parameters- S, F, and A —were systematically varied across different levels to evaluate their effects on these mechanical properties. For each experimental trial, measurements of tensile strength and hardness were obtained, and the corresponding S/N ratios were calculated to quantify performance variations under varying conditions. The experimental results demonstrate a significant influence of these parameters on both tensile strength and hardness. For instance, Run 5, characterized by a S of 900 rpm, a F of 40 mm/min, and a A of 6°, yielded the maximum tensile

Table 3. Taguchi L9 design, responses, and S/N ratios of the responses

Run	Parameter/Factor			Responses		S/N Ratio	
	Rotation speed (rpm)	Travel speed (mm/min)	Tool-pin taper (°)	Ts (Mpa)	Hv	Ts	Hv
1	800	20	0	176.06	72.50	44.91	37.21
2	800	40	3	183.71	73.82	45.28	37.36
3	800	60	6	189.06	78.42	45.53	37.89
4	900	20	3	196.24	82.06	45.86	38.28
5	900	40	6	215.40	90.69	46.66	39.15
6	900	60	0	190.81	74.45	45.61	37.44
7	1000	20	6	204.74	92.77	46.22	39.35
8	1000	40	0	191.35	83.70	45.64	38.45
9	1000	60	3	195.72	87.79	45.83	38.87

Table 4. Response table for signal-to-noise ratios for tensile strength and hardness

Level	Tensile strength			Hardness		
	S	F	A	S	F	A
1	45.24	45.66	45.39	37.49	38.28	37.70
2	46.04	45.86	45.66	38.29	38.32	38.17
3	45.90	45.66	46.14	38.89	38.06	38.80
Delta	0.80	0.20	0.75	1.40	0.26	1.10
Rank	1	3	2	1	3	2

Table 5. Analysis of variance for SN ratios of tensile strength

Source	DF	Seq SS	Adj SS	Adj MS	F	P	% Contribution
S	2	1.09325	1.09325	0.54663	40.39	0.024	52.17
F	2	0.07985	0.07985	0.03992	2.95	0.253	3.85
A	2	0.87342	0.87342	0.43671	32.26	0.030	42.11
Residual error	2	0.02707	0.02707	0.01354	0	0	1.31
Total	8	2.07360	0	0	0	0	100

S = 0.1163, R-Sq = 98.69%, R-Sq(adj) = 94.78%

Table 6. Analysis of variance for SN ratios of hardness test

Source	DF	Seq SS	Adj SS	Adj MS	F	P	% Contribution
S	2	2.9787	2.9787	1.48936	15.31	0.061	58.38
F	2	0.1145	0.1145	0.05724	0.59	0.630	2.24
A	2	1.8148	1.8148	0.90742	9.33	0.097	35.56
Residual error	2	0.1945	0.1945	0.09726	0	0	3.81
Total	8	5.1026	0	0	0	0	100

S = 0.3119, R-Sq = 96.19%, R-Sq(adj) = 84.75%

strength of 215.40 MPa and hardness of 90.69 HV, along with the highest S/N ratios of 46.66 for Ts and 39.15 for Hv. In contrast, Run 1, employing a lower rotation speed and smaller tool-pin taper angle, exhibited the lowest tensile strength (176.06 MPa) and hardness (72.50 HV), reflected in the lowest S/N ratios of 44.91 and 37.21, respectively. This comparative analysis highlights that an optimal combination of moderate rotation speed and larger tool-pin taper angle, as demonstrated in Run 5, results in enhanced mechanical performance. Therefore, these parameter settings may be considered optimal for maximizing the joint's tensile strength and hardness.

Table 4 presents a response analysis of the S/N ratios for tensile strength and hardness, based on varying levels of three critical parameters: S, F, and A. The levels correspond to different settings for each parameter, and the S/N ratios reflect the robustness of tensile strength and hardness against variations in these parameters. For tensile strength, the highest S/N ratios for each parameter were observed as follows: 46.14 at Level 3 of A, 45.90 at Level 3 of S, and 45.86 at Level 2 of F. The Delta values, representing the differences between the highest and lowest S/N ratios for

each factor, indicate that S has the most significant impact (Delta = 0.80), ranking it first in importance. This is followed by A with a Delta of 0.75 and F with a Delta of 0.20. Similarly, for hardness, the highest S/N ratios were observed at Level 3 of S with 38.89, Level 3 of A with 38.80, and Level 2 of F with 38.32. The Delta values for hardness further confirm that S exerts the most substantial influence (Delta = 1.40), followed by A with a Delta of 1.10 and F with a Delta of 0.26. Overall, this analysis identifies S as the most influential factor for optimizing both tensile strength and hardness in the Friction Stir Welding (FSW) process of AA5083-AA6063 alloys. A and F rank second and third, respectively. These findings suggest that careful optimization of rotation speed is crucial for achieving enhanced mechanical properties in the welded joints.

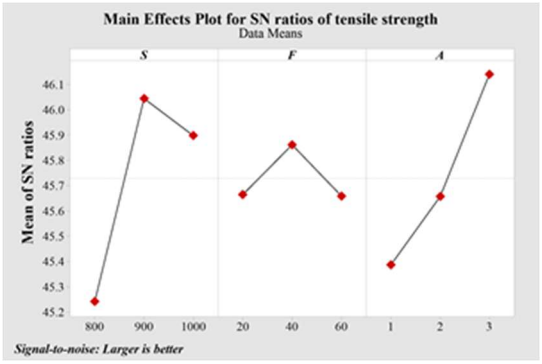

(a) Tensile strength

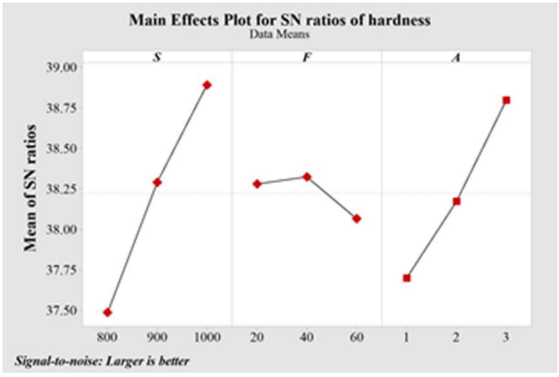

(b) Hardness

Fig. 3. Main Effects Plot for SN ratios

Tables 5 and 6 present the Analysis of Variance (ANOVA) results for the S/N ratios of tensile strength and hardness tests, respectively, aimed at optimizing the FSW process parameters. In Table 5, focusing on tensile strength, the S exhibits the highest percentage contribution at 52.17%, accompanied by a significant F- value of 40.39 and a p-value of 0.024. This underscores its strong influence on tensile strength. The A follows with a 42.11% contribution, an F-value of 32.26, and a p-value of 0.030, indicating a substantial effect. In contrast, the F has the lowest impact, contributing only 3.85% and yielding an F-value of 2.95 with a p-value of 0.253, suggesting it is not statistically significant. The residual error is minimal at 1.31%. The model demonstrates high explanatory power, evidenced by an R-squared (R^2) value of 98.69% and an adjusted R-squared (R^2_adj) of 94.78%, indicating that it accounts for the majority of the variation in tensile strength. Similarly, Table 6, which assesses hardness, reveals that rotation speed (S) again has the most significant impact, contributing 58.38% with an F-value of 15.31 and a p-value of 0.061. This suggests a strong influence on hardness. The A is the second most influential factor, with a contribution of 35.56%, an F-value of 9.33, and a p-value of 0.097, indicating a considerable effect. The F contributes minimally at 2.24%, with an F-value of 0.59 and a p-value of 0.630, rendering it statistically insignificant. The residual error stands at 3.81%. The model's effectiveness is further supported by an R-squared (R^2) of96.19% and an adjusted R-squared (R^2_adj) of 84.75%, indicating a strong ability to explain the variation in hardness. Overall, these ANOVA analyses confirm that S is the most critical factor influencing both tensile strength and hardness in the FSW process of AA5083-AA6063 alloys, followed by the A. The F has an insignificant effect on these mechanical properties. These findings highlight the importance of optimizing rotation speed and tool-pin taper angle to enhance the mechanical performance of FSW join(b) Hardness

Fig. 3 presents the main effects plots for the S/N ratios of tensile strength and hardness, illustrating the influence of each process parameter- S, F, and tool-pin taper angle (A)- on the mechanical properties of AA5083-AA6063 alloy joints during the FSW process. In Fig. 3(a), which pertains to tensile strength, the highest S/N ratio is observed at a rotation speed of 900 rpm, indicating that this parameter setting is optimal for maximizing tensile strength. The effect of F shows a peak at 40 mm/min, though the variations are relatively minimal compared to the impact of rotation speed. For the A, the maximum S/N ratio occurs at 6°, suggesting that a larger taper angle positively influences tensile strength. Similarly, Fig. 3(b), which addresses hardness, demonstrates that the S/N ratio reaches its maximum at a rotation speed of 900 rpm, underscoring the significant role of rotation speed in enhancing hardness. The influence of F on hardness is minimal, as indicated by the relatively flat response levels across different settings. However, the A exhibits an optimal value at 6°, akin to the tensile strength plot, indicating that a larger taper angle improves hardness. These main effects plots confirm that a S of 900 rpm and a A of 6° are critical parameters for optimizing both tensile strength and hardness in the FSW process. In contrast, F plays a relatively minor role in influencing these mechanical properties. This analysis aligns with the findings from the ANOVA tables, highlighting the importance of rotation speed and tool-pin taper angle in achieving desirable mechanical characteristics in AA5083-AA6063 alloy joints.

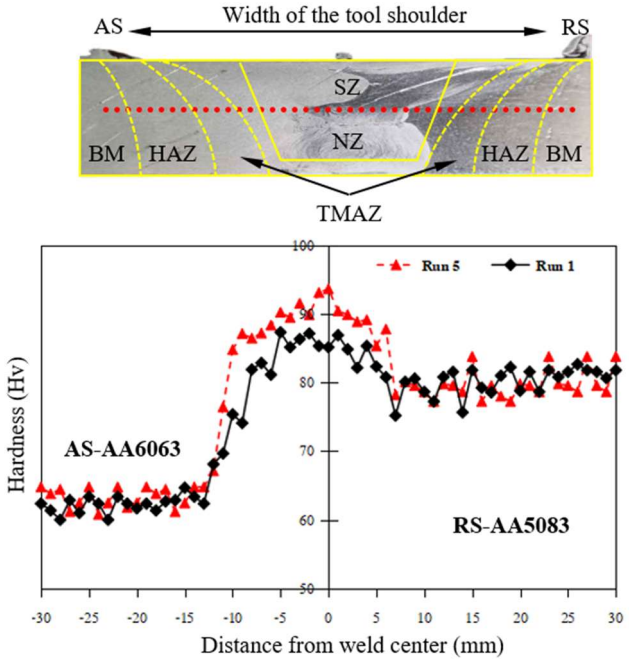

Fig. 4. The affected zone by the stirring process and the hardness testing positions.

3.2 Morphology of the Joint

In this section, a comparison is made specifically between the test specimen with the highest tensile resistance (Run 5-S900-F40-A6o) and the one with the lowest tensile resistance (Run 1-S800-F20-A0o). Fig. 4 illustrates the various zones affected during the FSW process and the specific locations where hardness testing was performed for the AA6063 (Advancing Side) and AA5083 (Retreating Side) alloys. The upper portion of the figure identifies distinct regions formed during welding, including the Base Material (BM), Heat-Affected Zone (HAZ), Thermo-Mechanically Affected Zone (TMAZ), and Stir Zone (SZ or Nugget Zone–NZ), along with the width influenced by the tool shoulder. NZ (Nugget Zone) is the central welding region characterized by severe plastic deformation and recrystallization, resulting in a fine-grained structure. The lower graph plots Hv against the distance from the weld center, comparing the results from Run 5 and Run 1. The hardness profiles reveal a significant increase near the weld center, peaking within the SZ. Run 5, represented by red triangles, exhibits a maximum hardness of approximately 95 Hv at the weld center, indicating superior hardness performance compared to Run 1, depicted by black diamonds, which reaches a peak hardness of around 85 Hv. The hardness levels decrease symmetrically as the distance from the weld center increases, stabilizing toward the base material values on both sides. This pattern confirms that the highest hardness is achieved in the SZ, with Run 5 demonstrating enhanced hardness properties over Run 1. These findings suggest that the optimized welding parameters employed in Run 5 effectively enhance the mechanical properties of the joint.

Fig. 5 provides a comparative analysis of the joint surface and macrostructure within the SZ for Run 5 and Run 1, highlighting notable differences in quality and structural characteristics. In panel (a) representing Run 5, the joint surface appears smooth and uniform, with a well-defined SZ width of 16 mm. The macrostructural image reveals a homogeneous microstructure within the SZ, indicating effective material mixing and thermal stability on both the AS and RS This uniformity suggests that the optimized FSW parameters employed in Run 5 have contributed to the formation of a strong and consistent joint. In contrast, panel (b) corresponding to Run 1 displays a joint surface that is less smooth and exhibits irregularities, including visible defects along the SZ. The macrostructural analysis reveals an inhomogeneous structure within the SZ, characterized by poor mixing between the AS and RS. Such inhomogeneities are indicative of suboptimal process parameters in Run 1, which could lead to diminished mechanical properties and inconsistent joint quality. These comparative findings demonstrate that the parameters utilized in Run 5 resulted in a superior joint quality with a homogeneous microstructure, whereas Run 1 exhibited defects and structural inhomogeneities. This underscores the critical importance of optimizing FSW parameters to achieve desirable mechanical properties and joint integrity in the welding of AA5083-AA6063 alloys.

In the investigation of friction stir welding between AA5083 and AA6063, Fig. 6(a) reveals a uniformly refined and recrystallized grain structure indicative of superior material mixing and effective precipitation hardening, which correlates with higher tensile strength. Conversely, Fig. 6(b) exhibits a heterogeneous grain structure with evident porosity and incoherent particulate agglomerations, suggesting suboptimal material flow and incomplete bonding. These microstructural deficiencies compromise the weld quality and result in a lower tensile performance. This comparison highlights the necessity for precise control of welding parameters to achieve an optimal balance in microstructural evolution and mechanical properties in dissimilar aluminum joints.

Fig. 7 illustrates the fracture surfaces obtained from tensile strength testing of the AA6063-AA5083 joint, comparing the outcomes of Run 5 (S900-F40-A6°) and Run 1 (S800- F20-A0°). In Fig. 6(a), corresponding to Run 5, the fracture surfaces on both the AS of AA6063 and the RS of AA5083 exhibit a "dimple surface" morphology, characteristic of ductile fracture. The uniform distribution of dimples indicates substantial plastic deformation and efficient energy absorption during fracture, contributing to enhanced joint strength and toughness. This fracture pattern suggests that the optimized FSW parameters employed in Run 5 facilitated robust interfacial bonding between the materials, resulting in desirable mechanical properties. In contrast, Fig. 6(b), representing Run 1, displays fracture surfaces with more heterogeneous characteristics. On the

Advancing Side of AA6063, the surface exhibits a combination of dimples and "cleavage" features, which are typically associated with brittle fracture mechanisms. The Retreating Side of AA5083 reveals "micro-cave" formations alongside dimples, indicating incomplete bonding and reduced energy
absorption during fracture. These observations suggest that the parameter settings in Run 1 resulted in weaker interfacial bonding and a more brittle fracture behavior, potentially diminishing the joint's overall mechanical performance. This comparison highlights that the optimized parameters in Run 5 produced a more homogeneous and ductile fracture morphology, while the parameters in Run 1 led to a mixed and less favorable fracture pattern. These findings underscore the critical importance of selecting appropriate FSW parameters to enhance joint performance and achieve desirable mechanical characteristics in AA6063-AA5083 welded joints.

4. DISSCUSION

The study's findings on optimized FSW parameters for AA5083-AA6063 alloy joints reveal a substantial impact of parameter selection on mechanical isolating rotation speed as the primary influential factor,with tool-pin taper angle following closely (Patel et al., 2019; Dharani and Sendhil, 2019). The moderate rotation speed coupled with a larger tool-pin taper angle outperformed other settings, achieving superior tensile strength and hardness by enhancing material mixing and joint homogeneity (Abdulhasan et al., 2020; Balamurugan et al., 2023). The role of tool-pin taper angle was evident in promoting effective material flow within the stir zone, which is essential for creating homogeneous joints A larger taper angle facilitated better material consolidation, resulting in a defect-free and uniform microstructure (Kumar and Chander, 2020; Nopriantoko, 2023). This setup not only contributed to the joint's strength but also provided consistency in hardness along the weld zone. The superior mechanical properties observed at the moderate rotation speed of 900 rpm can be attributed to a balanced thermal input that promotes effective material flow without causing overheating, which is further supported by the microstructural evidence shown in Fig. 5 and Fig. 6. At this speed, the frictional heat is sufficient to plasticize both AA5083 and AA6063, enabling thorough mixing in the stir

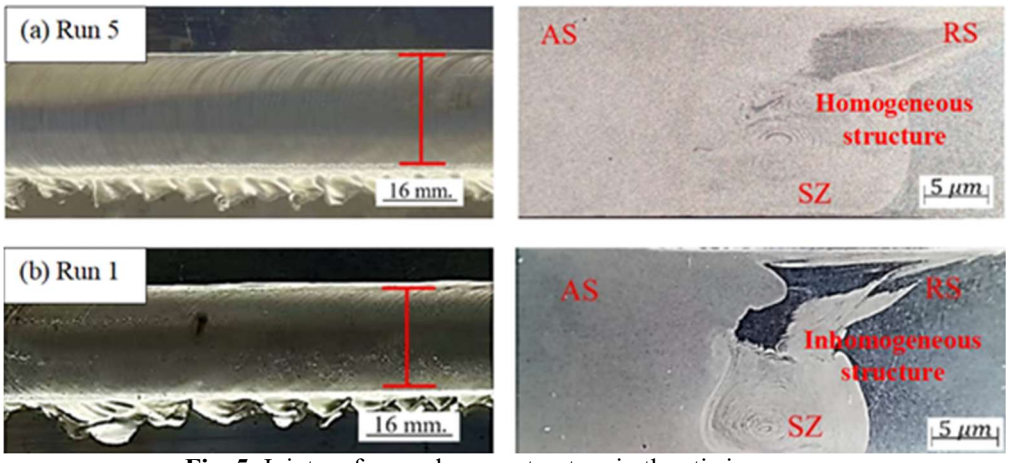

Fig. 5. Joint surface and macrostructure in the stirring zone.

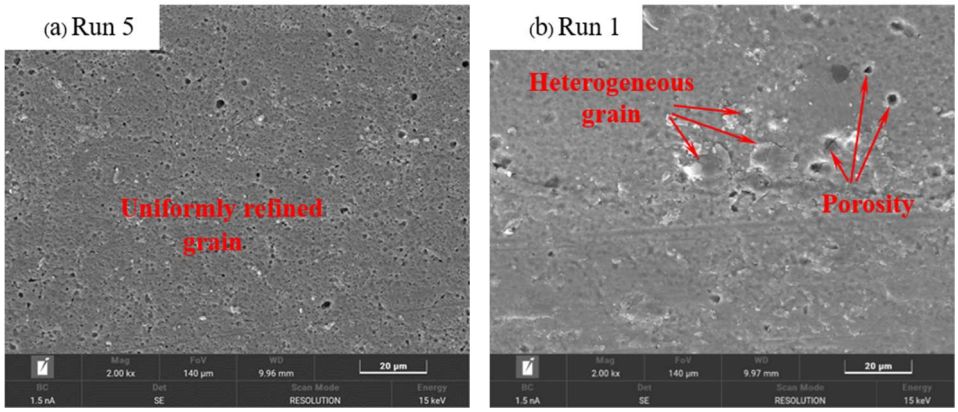

Fig. 6. Microstructure of AA5083 and AA6063 aluminum alloy joints (a) Run 5 (S900-F40-A6°) and (b) Run 1 (S800-F20-A0°)

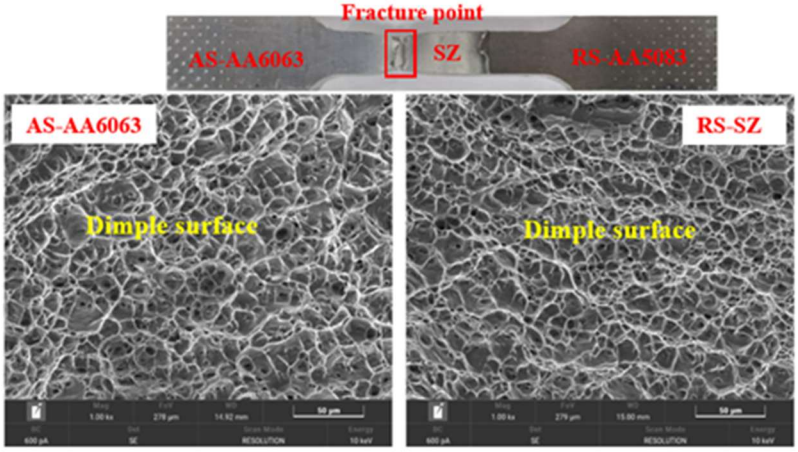

(a) Run 5 (S900-F40-A6°)

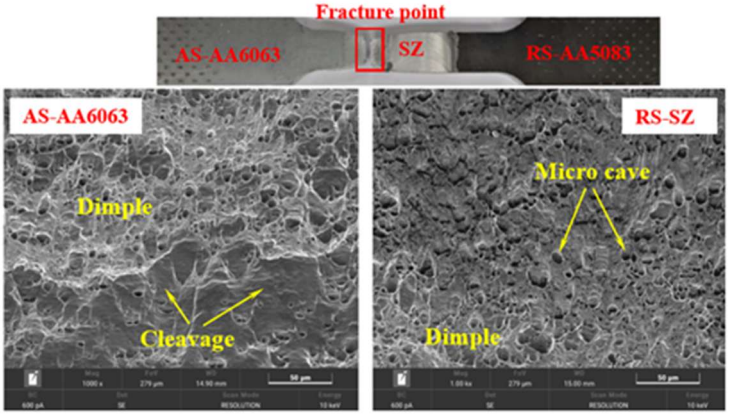

(b) Run 1 (S800-F20-A0°)

Fig. 7. Fracture surface from tensile strength testing.

zone while avoiding excessive grain coarsening. Higher rotation speeds (e.g., 1000 rpm) tend to introduce too much heat, leading to reduced strength due to grain growth and potential softening of the material. Conversely, lower speeds (e.g., 800 rpm) may not generate adequate heat, resulting in poor plastic flow and the formation of internal defects such as voids or lack of bonding. The stir zone in Run 5 (S900-F40-A6°) exhibited a fine and equiaxed grain structure with high homogeneity, while the fracture surface revealed uniformly distributed dimples on both advancing and retreating sides-indicative of ductile failure and strong interfacial bonding. In contrast, Run 1 (S800-F20-A0°) showed an inhomogeneous stir zone with visible voids and an uneven macrostructure. The corresponding SEM fracture images also exhibited cleavage facets and micro-cavities, suggesting brittle behavior and insufficient material flow. These findings confirm that the moderate setting provides an optimal balance between heat input, stirring action, and material consolidation-resulting in finer microstructures, stronger joints, and improved joint integrity. Comparatively, previous FSW studies on aluminum alloys focused on similar parameters but often lacked the integrated approach used here, particularly the combination of Taguchi optimization and detailed fracture analysis, underscoring this study's novel contributions (Patel et al., 2019; Balamurugan et al., 2023;). Microstructural and fracture morphology analyses validated the robustness of the optimized parameters. Observations revealed a ductile fracture pattern with uniformly distributed dimples, indicating strong interfacial bonding and effective energy absorption under stress. This contrasts with less optimized conditions, where irregularities and brittle features were observed, demonstrating weaker bonding (Patel et al., 2019; Kumar and Chander, 2020). The optimized FSW parameters hence not only enhanced mechanical properties but also ensured consistency in joint quality, marking a significant advancement in welding methodologies for AA5083-AA6063 alloys.

5. CONCLUSSION

In this study, we optimized FSW parameters to enhance the mechanical properties of AA5083-AA6063 aluminum alloy joints, addressing the critical need for robust welding techniques in manufacturing. Utilizing a Taguchi L9

orthogonal array design, rotation speed, travel speed, and tool-pin taper angle were systematically varied to assess their impact on joint performance. The results identified rotation speed as the most influential factor, followed by tool-pin taper angle, with travel speed having minimal effect. An optimal combination of moderate rotation speed and a larger tool-pin taper angle achieved the highest tensile strength (215.40 MPa) and hardness (90.69 HV). Microscopic analysis confirmed the formation of defect-free welds with ductile fracture patterns, emphasizing the importance of precise parameter control in achieving superior joint quality. These findings offer practical guidance for optimizing FSW processes in manufacturing contexts. Future research could explore additional factors such as cooling conditions or different alloy combinations, potentially broadening the applicability of these results to industries like automotive and aerospace, where high-strength and durable aluminum alloy joints are essential. For future research, it is recommended to investigate the incorporation of reinforcement particles such as TiO_2 or SiC into the stir zone to further enhance joint performance. Additionally, corrosion behavior of dissimilar AA5083-AA6063 joints should be evaluated under various environmental conditions to support applications in marine and structural industries. The integration of advanced modeling techniques, such as Response Surface Methodology (RSM) or Artificial Neural Networks (ANN), may also offer deeper insight into parameter interactions and predictive control.

ACKNOWLEDGMENT

The authors would like to express their sincere appreciation to the Faculty of Industrial Technology and the Faculty of Engineering at Nakhon Phanom University, and the Faculty of Engineering at Khon Kaen University, for their generous support in providing access to the testing laboratories. Their assistance played a crucial role in the successful completion of this research.

REFERENCES

Abdulhasan, A., Challoob, S.H., Abdulrehman, M., 2020. Studying the mechanical and numerical properties of friction stir welding (FSW) for 6005 aluminum alloys. IOP Conference Series: Materials Science and Engineering, 870, 012141.

Al-Sabur, R., 2021. Tensile strength prediction of aluminium alloys welded by FSW using response surface methodology–Comparative review. Materials Today: Proceedings, 47, 1001–1007.

Arun, M., Muthukumaran, M., Balasubramanian, S., 2021. Tribological characterization of friction stir welded dissimilar aluminum alloy AA6061–AA5083 reinforced with CeO_2 and La_2O_3 nanoparticles. Industrial Lubrication and Tribology, 73, 431–439.

Balamurugan, A., Bhuvaneswari, M., Suresh, K., Sudha, M., 2023. Investigation on the mechanical properties of FSWed AA6063–T351 aluminum alloy joints. Materials Today: Proceedings, 72, 553–559.

Dharani Kumar, S., Sendhil Kumar, S., 2019. Investigation of mechanical behavior of friction stir welded joints of AA6063 with AA5083 aluminum alloys. Manufacturing and Materials Engineering, 23, 59–67.

Elatharasan, G., Manikandan, R., Karthikeyan, G., 2020. Multi-response optimization of process parameters in friction stir welding of dissimilar aluminum alloys by Grey relation analysis (AA 6061-T6 & AA5083-H111). Materials Today: Proceedings, 33, 1720–1724.

Elnabi, M.M.A., Elshalakany, A.B., Abdel-Mottaleb, M., Osman, T., Mokadem, A., 2019. Influence of friction stir welding parameters on metallurgical and mechanical properties of dissimilar AA5454–AA7075 aluminum alloys. Journal of Materials Research and Technology, 8, 2364–2376.

Kumar, P.S., Chander, M., 2020. Effect of tool pin geometry on FSW dissimilar aluminum alloys - (AA5083 & AA6061). Materials Today: Proceedings, 39, 472–477.

Lewise, K.A.S., Dhas, J.E.R., Pandiyarajan, R., Sabarish, S., 2023. Metallurgical and mechanical investigation on FSSWed dissimilar aluminum alloy. Journal of Advanced Joining Processes, 4, 100010.

Nopriantoko, R., 2023. Energy absorption and toughness analysis on FSW butt joint of AA 5052 and AA 5083. Politeknik Journal of Mechanical Engineering, 21, 4107.

Okubo, M., Kon, T., Abe, N., 2007. Mechanical properties of aluminum-based dissimilar alloy joints by power beams, arc and FSW processes. Journal of High Temperature Society, 33(4), 208–216.

Patel, V.V., Li, W., Wang, G., Wang, F., Vairis, A., Niu, P., 2019. Friction Stir Welding of dissimilar aluminum alloy combinations: State-of-the-Art. Metals, 9(3), 270.

Serier, M., Berrahou, M., Tabti, A., Bendaoudi, S., 2019. Effect of FSW welding parameters on the tensile strength of aluminum alloys. Applied Mechanics and Materials, 39, 41–48.

Umanath, K., Palanikumar, K., Sankaradass, V., Uma, K., 2021. Optimizations of friction stir welding process parameters of AA6063 Aluminium alloy by Taguchi technique. Materials Today: Proceedings, 46, 2006–2010.